Editors' Suggestion

Nanosecond-Scale Proton Emission from Strongly Oblate-Deformed ^{149}Lu

K. Auranen,[1,*] A. D. Briscoe,[1] L. S. Ferreira,[2] T. Grahn,[1] P. T. Greenlees,[1] A. Herzáň,[3] A. Illana,[1] D. T. Joss,[4] H. Joukainen,[1] R. Julin,[1] H. Jutila,[1] M. Leino,[1] J. Louko,[1] M. Luoma,[1] E. Maglione,[2] J. Ojala,[1] R. D. Page,[4] J. Pakarinen,[1] P. Rahkila,[1] J. Romero,[1,4] P. Ruotsalainen,[1] M. Sandzelius,[1] J. Sarén,[1] A. Tolosa-Delgado,[1] J. Uusitalo,[1] and G. Zimba[1]

[1]*Accelerator Laboratory, Department of Physics, University of Jyväskylä, FI-40014 Jyväskylä, Finland*

[2]*Centro de Física e Engenharia de Materiais Avançados CeFEMA, Instituto Superior Técnico, Universidade de Lisboa, Avenida Rovisco Pais, P1049-001 Lisbon, Portugal*

[3]*Institute of Physics, Slovak Academy of Sciences, SK-84511 Bratislava, Slovakia*

[4]*Department of Physics, Oliver Lodge Laboratory, University of Liverpool, Liverpool L69 7ZE, United Kingdom*

(Received 15 December 2021; revised 2 February 2022; accepted 22 February 2022; published 16 March 2022)

Using the fusion-evaporation reaction ^{96}Ru(^{58}Ni, $p4n$)^{149}Lu and the MARA vacuum-mode recoil separator, a new proton-emitting isotope ^{149}Lu has been identified. The measured decay Q value of 1920(20) keV is the highest measured for a ground-state proton decay, and it naturally leads to the shortest *directly* measured half-life of 450^{+170}_{-100} ns for a ground-state proton emitter. The decay rate is consistent with $l_p = 5$ emission, suggesting a dominant $\pi h_{11/2}$ component for the wave function of the proton-emitting state. Through nonadiabatic quasiparticle calculations it was concluded that ^{149}Lu is the most oblate deformed proton emitter observed to date.

DOI: 10.1103/PhysRevLett.128.112501

The study of particle radiation is one of the fundamental cornerstones of nuclear physics. For example, the process of α-particle emission has been studied since the dawn of modern physics [1,2], yet it took nearly three decades before Gamov [3], and independently Gurney and Condon [4], were able to describe how the helium nucleus is able to penetrate through the Coulomb and centrifugal barriers that in the classical picture prevent the escape of the α particle from the vicinity of the core. Their work can be seen as one of the fundamental breakthroughs supporting the probabilistic interpretation of quantum mechanics. The calculation of quantum mechanical tunneling through the barrier is relatively simple, but a proper modeling of α decay should address the very complex preformation of the α particle. The situation is simpler in the emission of a single constituent nucleon, such as proton decay. Although the first idea of proton emission was made early [5], the first undisputed evidence of it was not found until the early 1970s when a weak proton decay branch was observed from the $19/2^-$ isomeric state of ^{53}Co [6–8]. Nearly a decade had to pass before the discovery of ^{151}Lu [9], the first reported ground-state proton emitter. Detailed reviews of the experimental proton-emitter data can be found, for example, from Refs. [10–14].

Proton disintegration has the inviting feature that, in contrast to α decay, it is not necessary to address the preformation of the emitted cluster, which makes the theoretical handling of the decay process seemingly straightforward [15]. Proton decay is sensitive only to the energy released in the decay Q_p, the angular momentum carried by the proton l_p, and on the probability whether following the emission the child nucleus is in the ground state or in an excited state. This probability depends on the deformation of the system. The relatively simple phenomenological models, such as the Geiger-Nuttall–like models [16,17] or the low-seniority shell model [10,18], are usually capable of explaining the experimental data reasonably well by assuming a spherical parent nucleus, and accounting only for Q_p and l_p. For well-deformed proton emitters more sophisticated models, such as the nonadiabatic quasiparticle approach [19], are needed to account for the effects arising from the deformed shape. In addition to the standard quadrupole deformation parameter β_2, corresponding to pure prolate ($\beta_2 > 0$, "rugby ball shape") or oblate ($\beta_2 < 0$, "pumpkin shape") deformation, the model has been expanded [20] to cover more complex triaxial shapes. More recently, the model was extended into triaxially deformed odd-odd proton emitters [21] via the interpretation of the newly discovered proton-decay branch in ^{108}I [22], which was also found to play a role in the modeling of the termination of the astrophysical rp process [23]. Odd-odd proton emitters are particularly important as the odd neutron affects the angular momentum of the emitted proton, and therefore these nuclei represent a good laboratory to study the residual proton-neutron interaction.

In this Letter we report the discovery of ^{149}Lu; a new proton emitter with exceptional properties. In addition to having the highest thus far measured Q_p value, naturally leading to the shortest directly measured half-life of any ground-state proton emitter, we conclude via nonadiabatic

TABLE I. Theoretical predictions for the one proton separation energy ($S_p = -Q_p$) and ground-state deformation β_2 of ^{149}Lu.

Model	S_p (MeV)	β_2
RHB [29]	−1.77	−0.158
FRDM [30,31]	−1.52	−0.187
RMF [32]	−1.946	−0.166

quasiparticle calculations that it is likely to be the most oblate deformed proton emitter observed to date. The previous record holder was ^{151}Lu, the proton-emitting $11/2^-$ ground state of which Procter *et al.* [24] concluded to have a deformation of $\beta_2 = -0.11^{+0.02}_{-0.05}$ via lifetime measurements. Furthermore, for its proton-emitting isomeric $3/2^+$ state Taylor *et al.* [25] obtained very similar values of $\beta_2 = -0.11$ and $\beta_2 \approx -0.12$ from the excited state structure, and from the half-life of the isomer, respectively. More deformed proton emitters are known, but these are either triaxial (see, for example, ^{141}Ho [26,27]) or prolate deformed (^{131}Eu, Ref. [28] and references therein). For ^{149}Lu different theoretical models predict a significantly larger oblate deformation than that of ^{151}Lu; see Table I for results obtained via the relativistic Hartree-Bogoliubov model (RHB [29]), finite-range droplet model (FRDM [30,31]), and deformed relativistic mean field theory (RMF [32]). These models appear to be consistent with the significant oblate deformation, although they predict rather different proton-separation energies S_p. This is the first instance when the theoretical models of proton disintegration are tested against such a high oblate deformation. Reliable calculations of the proton-emission process from oblate nuclei are crucial, for example, for the modeling of the astrophysical rp process as the swift proton emission of presumably oblate-deformed [30] ^{69}Br and ^{73}Rb nuclei create waiting points at ^{68}Se and ^{72}Kr. It is possible to bypass a waiting point with a direct $2p$ capture, the rate of which depends exponentially on S_p, making the accurate spectroscopic information and theoretical predictions a crucial input for the models of nuclear astrophysics.

A fusion-evaporation reaction ^{96}Ru(^{58}Ni, $p4n$)^{149}Lu with a five particle nA (3×10^{10} ions/s) beam intensity, provided by the K130 cyclotron of University of Jyväskylä, was used to produce the nuclei of interest. Beam energies of 310 and 320 MeV were used over an exposure times of 21 and 24 h, respectively. Furthermore, a beam energy of 267 MeV was used to produce ^{151}Lu [$E_p = 1233(3)$ keV [33]] in the $p2n$ evaporation channel to calibrate the response (offset parameter) of the implantation detector. Additionally, known α emitters ^{150}Dy, ^{152}Er, ^{154}Yb, and ^{155m,156m}Lu were used to obtain the gain parameter of the linear energy calibration. The target contained a 170-μg/cm^2 thick layer of enriched ^{96}Ru isotope evaporated on a beam-facing aluminum foil with a thickness of 150 μg/cm^2. Around the target position, scintillation detectors (Jyväskylä-York Tube, JYTube) were mounted in a barrel geometry to detect evaporated charged particles. After the target the evaporation residues, referred to as recoils hereafter, were separated from the primary beam and other unwanted beam- and targetlike ions in the Mass Analyzing Recoil Apparatus (MARA [34,35]). At the focal plane of MARA the horizontal position of recoils, corresponding to different mass-to-charge state ratios A/q, were measured with a multiwire proportional counter (MWPC). The MARA reference was set to $A = 149$ and $q = +28.5$ ($q = +29.5$) for the beam energy of 310 MeV (320 MeV). In practice, four charge states were collected at the same time. Additionally, the MWPC allowed the separation of recoils from scattered beam via the MWPC-implantation detector time of flight and the measured energy of the implantation events. After the MWPC, the recoils were implanted into a 159-μm thick double-sided silicon strip detector (DSSD) consisting of 192×72 strips with a pitch of 670 μm. As the proton decay of ^{149}Lu is predicted to be very fast, a 5-μs long wave form sample (trace) of each event was recorded from the X side of the DSSD. Delayed γ rays were detected with three broad-energy germanium (BEGe) detectors placed in close geometry around the focal-plane vacuum chamber. Data from all detectors were recorded independently and time stamped with a 100 MHz clock, which is also the sample rate of the recorded traces. The data were sorted and analyzed using the GRAIN software package [36].

Altogether 14 fast decay events, which we attribute to the proton disintegration of ^{149}Lu, were recorded in the same pixel of the DSSD as the preceding recoil-implantation event. The events were partitioned equally for the two beam energies and their yield corresponds to an approximately 50 nb cross section. The Y side of the DSSD was used to ensure that the two events present in one trace truly happened in the same pixel. The recorded traces for two of these events are displayed in Fig. 1, see the Supplemental Material [37] for other traces and the respective decay data. The recoil implantation event is followed by a spurious oscillation on the recorded trace, and therefore a dead time of 300 ns was set in the software to avoid false decay events. The dead time is accounted for in the data analyses and is displayed as a gray region in Fig. 1.

The mass-over-charge state distribution of the candidates is shown in Fig. 2. For comparison, two A/q spectra with better statistics are provided. These were acquired by setting a gate on γ rays, measured using the focal plane BEGe detectors, which are from the deexcitation of the isomeric states in ^{149,150}Er [38,39] nuclei. It was found via the sum of squared residuals that the recoil preceding the fast proton decay most likely has a mass number of 149. Element assignment was carried out using the JYTube data, i.e., at the target position, zero or one evaporated charged particles correlated with the fast decaying residues,

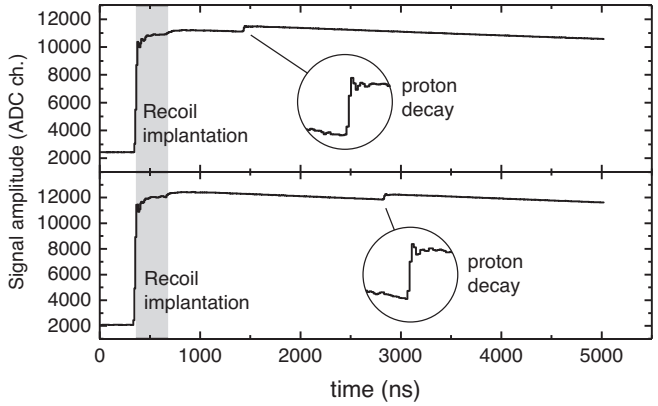

FIG. 1. Two examples of a wave form recorded for the fast proton decay of ^{149}Lu. The grey region marks a dead time set in software.

corresponding to a pxn evaporation channel. It should be noted that the hafnium (xn channel) or ytterbium ($2pxn$ or αxn channel) nuclides produced in the reaction have either negative or very small positive proton decay Q values [31], and can be therefore excluded. Proton-decay properties of similar-mass thulium isotopes are well known [12]. Neither the proton-decay energy nor the half-life of the new activity corresponds to known characteristics of the thulium isotopes, in particular ^{149}Tm does not decay via proton emission [40]. Therefore, we assign the new proton-decay activity to hitherto unknown nucleus ^{149}Lu.

The energy spectrum of the emitted protons associated with ^{149}Lu is shown in Fig. 3. A proton energy of 1910(20) keV was obtained as the arithmetic mean of the individual proton energies forming the characteristic peak shown in Fig. 3. The proton energy corresponds to a proton-decay Q value of 1920(20) keV, which is the highest ground-state

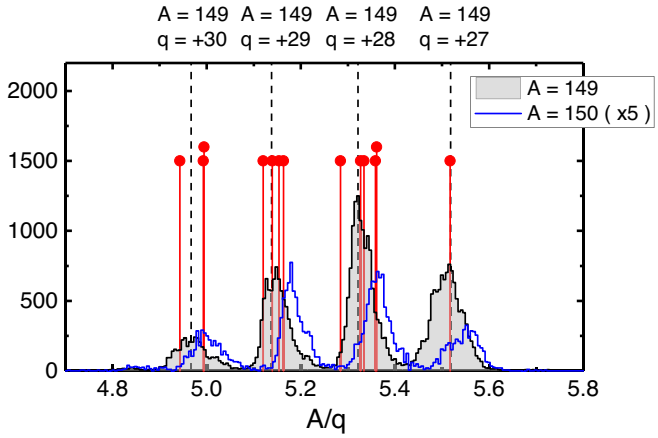

FIG. 2. Mass-over-charge state ratios of the ^{149}Lu candidates (red symbols). The dashed lines are the exact A/q ratios as indicated, and the solid distributions are for comparison. The reference spectra were obtained by gating with the γ rays from the deexcitation of the known 10^+ [38] ($19/2^+$ [39]) isomeric state in ^{150}Er (^{149}Er).

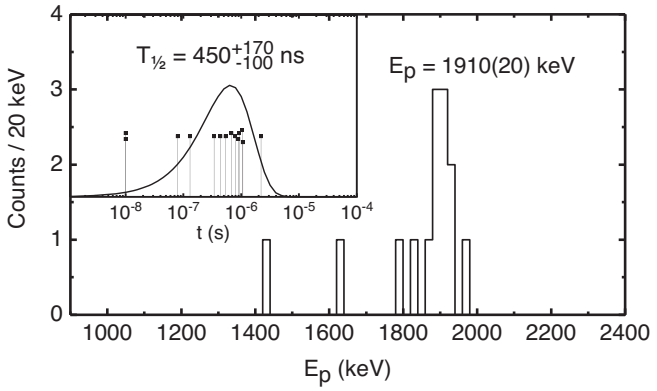

FIG. 3. Energy spectrum of the protons associated with the decay of ^{149}Lu. The inset displays the decay-time distribution of the protons. The half-life was extracted with the maximum likelihood method [46], and the solid line is the probability density distribution corresponding to the measured half-life.

proton-decay energy measured. Determination of the Q_p permits an immediate testing of the predictive power of the state-of-the-art atomic mass models on extremely neutron-deficient nuclei. In Fig. 4 the experimental Q_p values of selected nuclei close to the proton drip line are compared to the results of the KTUY05 atomic mass model, finite-range droplet model, average of six energy-density functional based theories, and relativistic mean field theory. Whereas the last reproduces the experimental data reasonably well, it is evident that all the other models have a tendency to underestimate the

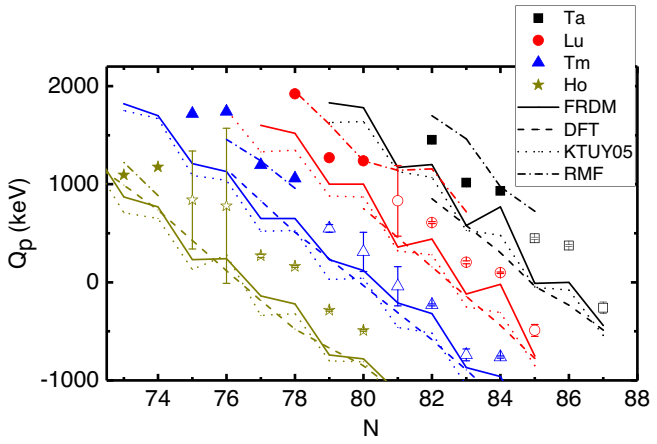

FIG. 4. Proton-decay Q value of selected tantalum (black), lutetium (red), thulium (blue), and holmium (olive green) nuclei. Experimental data for nuclei with a known proton-decay branch are indicated with solid symbols (this work and Ref. [12]), whereas open symbols denote other nuclei [47]. The lines show the predictions of different state-of-the-art theoretical models, namely, finite-range droplet model (solid line, [31]), energy-density functional theories [48] (dashed line, average of six models based on SkM* [49], SkP [50], SLy4 [51], SV-min [52], UNEDF0 [53], and UNEDF1 [54] functionals), KTUY05 atomic mass model (dotted line [55]), and the deformed relativistic mean field theory (dash-dotted line, [32]).

proton-decay energy. The divergence between theory and experiment is particularly large for the known proton-emitting (solid symbols) Tm, Lu, and Ta nuclei. A similar, but not as striking, divergence was found for the proton-unbound nuclei close to mass 210 in Ref. [41]. In addition, it is interesting to notice how the odd-even staggering gets more pronounced in the experimental data as one proceeds to the most exotic isotopes. This is due to the enhancement in the residual proton-neutron interaction as one is approaching the $N = Z$ line where the proton-neutron pairing should be the strongest. It is therefore possible that ^{148}Lu actually has a lower proton-decay Q value than ^{149}Lu, similar to the ^{140,141}Ho [42,43] and ^{144,145}Tm [44,45] counterparts, but this remains to be seen in the future experiments.

The decay time of a given event was defined as the time difference between the leading edges of the recoil-implantation event and the subsequent proton-decay event in the recorded trace, allowing for the dead time. The decay-time distribution of the 14 candidate events is shown in the inset of Fig 3. A half-life of 450^{+170}_{-100} ns was extracted via the maximum likelihood method of Ref. [46], and the solid line of the inset is the probability density distribution corresponding to this half-life. It is also noteworthy that the decay-time distribution passes the 90% probability test introduced in Ref. [56], thus these events are consistent with the assumption that they originate from the decay of a single radioactive species. As a consequence of the high decay energy, ^{149}Lu is the shortest-living ground-state proton emitter with a directly measured half-life. The Geiger-Nuttall type model of Chen *et al.* [17] predicts a proton-decay half-life of 956 ns for a $l_p = 5$ proton emitted with the present Q_p value. The measured half-life is within one standard deviation of the model. However, a more sophisticated theoretical treatment is needed to explain the experimental data fully.

Theoretical calculations to interpret the experimental results were performed within the nonadiabatic quasiparticle model [19]. The pairing residual interaction was taken into account in a consistent way, rather than using a spectroscopic factor. The BCS approach was used, and the Coriolis interaction was diagonalized between quasiparticle states. The excitation pattern of the child nucleus was included by coupling the odd proton to the experimental level structure of the even-even core. As there is no experimental information available for ^{148}Yb, the ^{148}Er nucleus, the yrast band of which deviates from that of an ideal rotor, was selected as the core. For the single-particle potential, the Esbensen and Davids parameterization [57] was used which has proved to work well in this mass region [24]. Within the model the possible candidates lying close to the Fermi surface are the $11/2^-$, $3/2^+$, and $1/2^+$ states, of which the last two can be excluded as their proton-decay rate diverges from the measured one by 3 and 4 orders of magnitude, respectively.

The half-life calculated with the nonadiabatic quasiparticle model, as a function of the quadrupole deformation, is compared to the measured half-life in Fig. 5. The finite-range droplet model [30] predicts a hexadecapole deformation of $\beta_4 = -0.043$ for ^{149}Lu, hence, the calculations were repeated for a hexadecapole deformation of $\beta_4 = 0$ (blue) and $\beta_4 = 0.225\beta_2$ (red). Particularly on the oblate side, the effect arising from the hexadecapole deformation was found to be negligible. A parabolic behavior was observed around the spherical shape, for which the wave function is the quasiparticle $h_{11/2}$ coupled to the 0^+ ground state of the core. Deformation brings other components of the quasiparticle states and of the core into play, reducing the $h_{11/2} \otimes 0^+$ component and slowing down the decay. The calculated half-life agrees with the measured one if the nucleus is significantly ($\beta_2 \lesssim -0.17$) oblate deformed. To the best of our knowledge, this is the largest oblate deformation ever assigned for a ground-state proton emitter. The limit is also very similar to the predictions in Table I. Furthermore, in agreement with the nonadiabatic quasiparticle model and experimental measurements for ^{151}Lu [24,25], other calculations made through the finite-range liquid drop model [58] as well as the Hartree-Fock-Bogoliubov calculations based on the D1S Gogny interaction [59,60] predict that ^{148}Yb (even-even core of ^{149}Lu) is more strongly oblate deformed than ^{150}Yb (^{151}Lu). This further supports the interpretation of ^{149}Lu being more strongly oblate deformed than ^{151}Lu. In principle the nonadiabatic quasiparticle model also agrees with a prolate deformation of $\beta_2 \approx 0.15$. However, it should be emphasized that no theoretical model predicts this for ^{149}Lu. The experimental evidence on the sign of β_2 would require

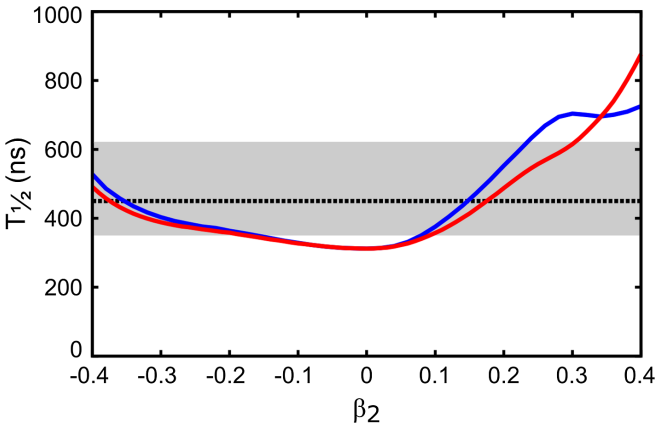

FIG. 5. The proton-decay half-life of ^{149}Lu as a function of the quadrupole deformation. The solid lines were calculated with the nonadiabatic quasiparticle model assuming Davids' potential [57] and a hexadecapole deformation of $\beta_4 = 0$ (blue) or $\beta_4 = 0.225\beta_2$ (red). The uncertainty of the calculated half-life, arising from the uncertainty of the measured Q_p, is approximately 20%. The dashed line together with the gray band denote the measured half-life.

measurement of the level spacing of the ground-state band. Based on our experience it should be feasible, but would be very challenging.

In summary, we have identified a new swift proton-emission activity that we attribute to the decay of $11/2^-$ state in ^{149}Lu based on the measured mass number and production channel of the recoiling nuclei. The highest ever measured ground-state proton-decay energy of 1920(20) keV is in good agreement with the Q_p systematics and relativistic mean field theory, but it was found that a majority of the state-of-the-art atomic mass models systematically overestimate the proton binding in this part of the chart of nuclides. To date, this shortest directly measured half-life of a ground-state proton emitter of 450^{+170}_{-100} ns is reproduced by the nonadiabatic quasiparticle calculations if the nucleus is strongly oblate deformed. In fact, the quadrupole deformation less than -0.17 is the most strongly oblate value assigned to a ground-state proton emitter thus far. In-beam γ-ray spectroscopy is needed for ^{149}Lu to resolve fully the question of extreme oblate deformation, which no doubt will be very challenging. Similarly demanding, yet still feasible, is to synthesize the new isotope ^{148}Lu that might conceivably be longer-lived than ^{149}Lu due to enhancement of the residual proton-neutron interaction driving to reduce the Q_p value.

This work was supported by the Academy of Finland under the Contract No. 323710 (Personal research project, K. A.). R. D. P. and D. T. J. acknowledge support of the Science and Technology Facilities Council, UK. A. H. would like to thank the Slovak Research and Development Agency under Contract No. APVV-20-0532, and Slovak grant agency VEGA (Contract No. 2/0067/21).

*kalle.e.k.auranen@jyu.fi

[1] E. Rutherford, Philos. Mag. **47**, 109 (1899).
[2] E. Rutherford, Nature (London) **64**, 157 (1901).
[3] G. Gamow, Z. Phys. **51**, 204 (1928).
[4] R. W. Gurney and E. U. Condon, Nature (London) **122**, 439 (1928).
[5] E. Marsden and W. C. Lantsberry, Philos. Mag. **30**, 240 (1915).
[6] J. Cerny, J. E. Esterl, R. A. Gough, and R. G. Sextro, Phys. Lett. B **33**, 284 (1970).
[7] K. P. Jackson, C. U. Cardinal, H. C. Evans, N. A. Jelley, and J. Cerny, Phys. Lett. B **33**, 281 (1970).
[8] J. Cerny, R. A. Gough, R. G. Sextro, and J. E. Esterl, Nucl. Phys. **A188**, 666 (1972).
[9] S. Hofmann, W. Reisdorf, G. Münzenberg, F. P. Heßberger, J. R. H. Schneider, and P. Armbruster, Z. Phys. A **305**, 111 (1982).
[10] P. J. Woods and C. N. Davids, Annu. Rev. Nucl. Part. Sci. **47**, 541 (1997).
[11] A. Sonzogni, Nucl. Data Sheets **95**, 1 (2002).
[12] B. Blank and M. J. G. Borge, Prog. Part. Nucl. Phys. **60**, 403 (2008).
[13] R. D. Page, EPJ Web Conf. **123**, 01007 (2016).
[14] C. Qi, R. Liotta, and R. Wyss, Prog. Part. Nucl. Phys. **105**, 214 (2019).
[15] D. S. Delion, R. J. Liotta, and R. Wyss, Phys. Rep. **424**, 113 (2006).
[16] D. S. Delion, R. J. Liotta, and R. Wyss, Phys. Rev. Lett. **96**, 072501 (2006).
[17] J.-L. Chen, J.-Y. Xu, J.-G. Deng, X.-H. Li, B. He, and P.-C. Chu, Eur. Phys. J. A **55**, 214 (2019).
[18] C. N. Davids, P. J. Woods, J. C. Batchelder, C. R. Bingham, D. J. Blumenthal, L. T. Brown, B. C. Busse, L. F. Conticchio, T. Davinson, S. J. Freeman, D. J. Henderson, R. J. Irvine, R. D. Page, H. T. Penttilä, D. Seweryniak, K. S. Toth, W. B. Walters, and B. E. Zimmerman, Phys. Rev. C **55**, 2255 (1997).
[19] G. Fiorin, E. Maglione, and L. S. Ferreira, Phys. Rev. C **67**, 054302 (2003).
[20] P. Arumugam, E. Maglione, and L. S. Ferreira, Phys. Rev. C **76**, 044311 (2007).
[21] P. Siwach, P. Arumugam, S. Modi, L. S. Ferreira, and E. Maglione, Phys. Rev. C **103**, L031303 (2021).
[22] K. Auranen *et al.*, Phys. Lett. B **792**, 187 (2019).
[23] H. Schatz, A. Aprahamian, V. Barnard, L. Bildsten, A. Cumming, M. Ouellette, T. Rauscher, F.-K. Thielemann, and M. Wiescher, Phys. Rev. Lett. **86**, 3471 (2001).
[24] M. G. Procter *et al.*, Phys. Lett. B **725**, 79 (2013).
[25] M. J. Taylor *et al.*, Phys. Rev. C **91**, 044322 (2015).
[26] P. Arumugam, L. S. Ferreira, and E. Maglione, Phys. Lett. B **680**, 443 (2009).
[27] S. Modi, M. Patial, P. Arumugam, L. S. Ferreira, and E. Maglione, Phys. Rev. C **96**, 064308 (2017).
[28] Yu. Khazov, I. Mitropolsky, and A. Rodionov, Nucl. Data Sheets **107**, 2715 (2006).
[29] G. A. Lalazissis, D. Vretenar, and P. Ring, Phys. Rev. C **60**, 051302(R) (1999).
[30] P. Möller, A. J. Sierk, T. Ichikawa, and H. Sagawa, At. Data Nucl. Data Tables **109–110**, 1 (2016).
[31] P. Möller, M. R. Mumpower, T. Kawano, and W. D. Myers, At. Data Nucl. Data Tables **125**, 1 (2019).
[32] L. Geng, H. Toki, and J. Meng, Prog. Theor. Phys. **112**, 603 (2004).
[33] B. Singh, Nucl. Data Sheets **110**, 1 (2009).
[34] J. Sarén, J. Uusitalo, M. Leino, P. T. Greenlees, U. Jakobsson, P. Jones, R. Julin, S. Juutinen, S. Ketelhut, M. Nyman, P. Peura, P. Rahkila, C. Scholey, and J. Sorri, Nucl. Instrum. Methods Phys. Res., Sect. B **266**, 4196 (2008).
[35] J. Uusitalo, J. Sarén, J. Partanen, and J. Hilton, Acta Phys. Pol. B **50**, 319 (2019).
[36] P. Rahkila, Nucl. Instrum. Methods Phys. Res., Sect. A **595**, 637 (2008).
[37] See Supplemental Material at http://link.aps.org/supplemental/10.1103/PhysRevLett.128.112501 for the recorded traces and the respective decay data.
[38] Y. H. Chung, P. J. Daly, H. Helppi, R. Broda, Z. W. Grabowski, M. Kortelahti, J. McNeill, A. Pakkanen, P. Chowdhury, R. V. F. Janssens, T. L. Khoo, and J. Blomqvist, Phys. Rev. C **29**, 2153 (1984).
[39] D. Nisius, R. V. F. Janssens, I. G. Bearden, R. H. Mayer, I. Ahmad, P. Bhattacharyya, B. Crowell, M. P. Carpenter, P. J. Daly, C. N. Davids, Z. W. Grabowski, D. J. Henderson,

R. G. Henry, R. Hermann, T. L. Khoo, T. Lauritsen, H. T. Penttilä, L. Ciszewski, and C. T. Zhang, Phys. Rev. C **52**, 1355 (1995).
[40] B. Singh, Nucl. Data Sheets **102**, 1 (2004).
[41] K. Auranen *et al.*, Phys. Rev. C **102**, 034305 (2020).
[42] K. Rykaczewski *et al.*, Phys. Rev. C **60**, 011301(R) (1999).
[43] C. N. Davids, P. J. Woods, D. Seweryniak, A. A. Sonzogni, J. C. Batchelder, C. R. Bingham, T. Davinson, D. J. Henderson, R. J. Irvine, G. L. Poli, J. Uusitalo, and W. B. Walters, Phys. Rev. Lett. **80**, 1849 (1998).
[44] R. Grzywacz, M. Karny, K. P. Rykaczewski, J. C. Batchelder, C. R. Bingham, D. Fong, C. J. Gross, W. Krolas, C. Mazzocchi, A. Piechaczek, M. N. Tantawy, J. A. Winger, and E. F. Zganjar, Eur. Phys. J. A **25**, 145 (2005).
[45] J. C. Batchelder *et al.*, Phys. Rev. C **57**, R1042 (1998).
[46] K. H. Schmidt, C. C. Sahm, K. Pielenz, and H. G. Clerc, Z. Phys. A **316**, 19 (1984).
[47] M. Wang, G. Audi, F. G. Kondev, W. J. Huang, S. Naimi, and X. Xu, Chin. Phys. C **41**, 030003 (2017).
[48] J. Erler, N. Birge, M. Kortelainen, W. Nazarewicz, E. Olsen, A. M. Perhac, and M. Stoitsov, Nature (London) **486**, 509 (2012).
[49] J. Bartel, P. Quentin, M. Brack, C. Guet, and H.-B. Håkansson, Nucl. Phys. **A386**, 79 (1982).
[50] J. Dobaczewski, H. Flocard, and J. Treiner, Nucl. Phys. **A422**, 103 (1984).
[51] E. Chabanat, P. Bonche, P. Haensel, J. Meyer, and R. Schaeffer, Nucl. Phys. **A635**, 231 (1998).
[52] P. Klüpfel, P.-G. Reinhard, T. J. Bürvenich, and J. A. Maruhn, Phys. Rev. C **79**, 034310 (2009).
[53] M. Kortelainen, T. Lesinski, J. Moré, W. Nazarewicz, J. Sarich, N. Schunck, M. V. Stoitsov, and S. Wild, Phys. Rev. C **82**, 024313 (2010).
[54] M. Kortelainen, J. McDonnell, W. Nazarewicz, P.-G. Reinhard, J. Sarich, N. Schunck, M. V. Stoitsov, and S. M. Wild, Phys. Rev. C **85**, 024304 (2012).
[55] H. Koura, T. Tachibana, M. Uno, and M. Yamada, Prog. Theor. Phys. **113**, 305 (2005).
[56] K. H. Schmidt, Eur. Phys. J. A **8**, 141 (2000).
[57] H. Esbensen and C. N. Davids, Phys. Rev. C **63**, 014315 (2000).
[58] P. Möller, A. J. Sierk, R. Bengtsson, H. Sagawa, and T. Ichikawa, At. Data Nucl. Data Tables **98**, 149 (2012).
[59] S. Hilaire and M. Girod, Eur. Phys. J. A **33**, 237 (2007).
[60] S. Hilaire and M.Girod, AMEDEE database, http://www-phynu.cea.fr/science_en_ligne/carte_potentiels_microscopiques/carte_potentiel_nucleaire_eng.htm, accessed 10.11.2021.